Am J Cancer Res 2024;14(5):2202-2215
www.ajcr.us /ISSN:2156-6976/ajcr0155465

Original Article

ITM2A inhibits the progression of bladder cancer by downregulating the phosphorylation of STAT3

Jiahao Jiang[1,2,3*], Jinming Xu[3*], Longhua Ou[3*], Cong Yin[3], Yan Wang[4], Bentao Shi[1,2,3]

[1]Department of Urology, Shenzhen Second People's Hospital, Clinical College of Anhui Medical University, Shenzhen, Guangdong, P. R. China; [2]The Fifth Clinical Medical College of Anhui Medical University, Hefei, Anhui, P. R. China; [3]Department of Urology, Shenzhen Second People's Hospital/The First Affiliated Hospital of Shenzhen University, Shenzhen, Guangdong, P. R. China; [4]Department of Urology, Peking University Shenzhen Hospital, Institute of Urology, Shenzhen PKU-HKUST Medical Center, Shenzhen, Guangdong, P. R. China. [*]Equal contributors.

Received January 15, 2024; Accepted April 29, 2024; Epub May 15, 2024; Published May 30, 2024

Abstract: Bladder cancer stands as one of the prevalent malignancies in urological clinics, highlighting the pressing need to uncover prognostic or therapeutic avenues. ITM2A, a transmembrane protein, has been identified as a suppressor in tumor progression recently. Our study underscored a significant correlation between low ITM2A expression in bladder cancer tissues and high tumor grade, AJCC stage, and poor overall survival time. Additionally, our findings demonstrated that reinstating ITM2A expression impeded cell proliferation, migration, and invasion, while conversely, its suppression enhanced these malignant behaviors. Furthermore, we elucidated that ITM2A could suppress malignant phenotypes of bladder cancer cells via inhibiting activation of the STAT3 induced by IL-6. In conclusion, our research unveiled the mechanistic role of ITM2A in inhibiting tumor progression, shedding light on its potential as a prognostic predictor and therapeutic target in bladder cancer management.

Keywords: ITM2A, bladder cancer, phosphorylation of STAT3, cell progression, tumor suppressor

Introduction

Bladder cancer (BLCA) ranks as the tenth most prevalent cancer globally, with approximately 573,000 newly diagnosed patients in 2020 [1]. Notably, approximately 70% of BLCA cases are diagnosed as non-muscle-invasive bladder cancer (NMIBC), typically managed through surgical intervention and postoperative perfusion [2]. Therefore, unraveling potential molecular mechanisms and identifying key biomarkers crucial to the pathogenesis of BLCA is imperative for enhancing therapeutic efficacy.

Among the six major proteins within the STAT family, STAT3 emerges as a significant member - a latent cytoplasmic transcription factor pivotal in cytokine-activated gene expression [3, 4]. Upon, ligand binding to cell surface receptors, STAT3 undergoes phosphorylation, dimerization, and nuclear translocation [5]. While this process is typically transient and tightly controlled, abnormal STAT3 hyperactivation is prevalent in various malignancies, including BLCA [6]. Persistent STAT3 activation in BLCA has been shown to facilitate cell proliferation, promote metastasis, and enhance chemoresistance [7]. Notably, STAT3 inhibition has been proven to successfully suppress BLCA progression both in vitro and in vivo [8], offering a promising avenue for novel therapeutic interventions.

ITM2A, a 263-amino acid transmembrane protein belonging to the type II integral membrane protein family, shares lineage with ITM2B and ITM2C [9]. Initially identified in a genomic library of BALB/c liver, the ITM2A gene is mapped to mouse chromosome position XA2-XA3 and human chromosome position Xq21.1, demonstrating high conservation between mouse and human [10]. Structurally, the ITM2A protein comprises four distinct regions: the hydrophobic domain, the linker region, the extracellular BRICHOS domain, and the intracellular domain [11]. Recent research has implicated ITM2A in various biological activities, including the regulation of cellular autophagic flux, cartilage dif-

https://doi.org/10.62347/KHCC9690

ferentiation, and tissue lipid metabolism [12-14]. In addition, the low expression of ITM2A in breast, ovarian, and cervical cancer tissues has been associated with poorer prognosis and advanced tumor stage [15-18]. However, the role and expression level of ITM2A in BLCA remain unknown.

Here, we observed the expression of ITM2A in BLCA tissues and cell lines, shedding light on its involvement in BCLA progression. ITM2A expression was negatively associated with clinicopathological characteristics, displaying significant downregulation in BLCA tissues and cell lines. Furthermore, restoration of ITM2A exhibited a pronounced inhibitory effect on cell proliferation, migration, and invasion on BLCA, along with a marked suppression of STAT3 phosphorylation. This research unveiled an innovative molecular mechanism whereby ITM2A inhibited BLCA progression, potentially paving the way for novel diagnostic and therapeutic strategies in managing this challenging disease.

Methods and materials

Database mining and patient collection

To compare ITM2A expression between BLCA and normal bladder tissues, the data for mRNA expression were obtained from The Cancer Genome Atlas (TCGA, https://tcga-data.nci.nih.gov/tcga) database and Gene Expression Omnibus (GEO, https://www.ncbi.nlm.nih.gov/geo/) database.

Forty pairs of tumor and adjacent normal bladder tissues were obtained from BLCA patients during surgery at the Department of Urology, Peking University Shenzhen Hospital. All fresh tissues were immediately immersed in RNA stabilization reagent (Beyotime, Shanghai, China) and then stored at -80°C. All patients were informed and signed written informed consent.

Cell culture and authentication

SV-HUC-1 and human BLCA cell lines (SW780, T24, UMUC-3, J82, 5637, and TCCSUP) were obtained from the American Type Culture Collection (Manassas, VA, USA). SV-HUC-1, transformed from normal human urothelial cells, was used as a control group for bladder cancer cell lines. Each cell line was tested and authenticated by Meisen Cell Technology Co., Ltd. (Hangzhou, China) on 4 July 2023. Cell lines were authenticated using short tandem repeat analysis as described in 2021 in ANSI Standard (ASN-0002) by the ATCC Standards Development Organization. BLCA cell lines were cultured in DMEM medium or RPMI-1640 medium (Gibco, Carlsbad, CA, USA), while the SV-HUC-1 cell line thrived best in Ham's F-12K (Kaighn's) medium (Gibco, Carlsbad, CA, USA). Each culture medium was supplemented with 10% fetal bovine serum (FBS, Gibco, Carlsbad, CA, USA) and 100 U/mL penicillin-streptomycin. Cells were maintained in a standard cell culture environment at 37°C with 5% CO_2.

Lentivirus infection and transfection

Lentiviruses carrying full-length ITM2A sequences and matched negative controls were constructed by Genechem Co., Ltd. (Suzhou, China). Upon reaching 20% confluence in a 12-well plate, T24 and UMUC-3 cells were exposed to the respective lentiviral particle solutions. Following a 72-hour incubation period, the culture medium was supplemented with 5 μg/mL puromycin to facilitate the generation of stable transfectants.

The T24 and SW780 cells were transfected with siRNAs using Lipofectamine 3000 (Invitrogen, Carlsbad, CA, USA) when the confluence reached 30%. ITM2A-specific siRNAs and negative control siRNAs were synthesized by GenePharma Co., Ltd. (Suzhou, China) and the antisense sequences (5'-3') were as follows: ITM2A siRNA-1: AUGAAUAAUUGCUGCAGGGTT; ITM2A siRNA-2: AACCACAUAAGUUUGAGGCTT.

Immunohistochemistry staining (IHC)

Single spot tissue microarray (TMA) slides (93 cases of BLCA, 46 cases of adjacent normal bladder tissues, HBlaU079Su01 and HBlaU060CS02, Shanghai Outdo Biotech Company, Shanghai, China) were prepared. The anti-ITM2A (106889-T40, 1:2000, Sino Biological Inc., China) was used for staining. According to the staining intensity (0 (negative), 1+, 2+, and 3+) and the staining positive rate (0-100%), two experienced pathologists evaluated the results. Then, the total score (0, 1, 2, 3, 4, 6, 8, 9, and 12) was calculated as the product of the staining intensity score and positive staining rate score. Samples with a total score of 4 or less were categorized into the low-expression group, while those with a score

higher than 4 were classified into the high-expression group.

RNA extraction and reverse transcription-quantitative PCR (RT-qPCR)

The method of RNA extraction and reverse transcription-quantitative PCR (RT-qPCR) followed our previous protocols [19]. In this process, the following reagents were used: TRIzol reagent (Invitrogen, Carlsbad, CA, USA), PrimeScript™ RT Reagent Kit (Takara, Japan), and SYBR Premix Ex Taq™ II Kit (Takara, Japan). The primers used in this study were as follows: ITM2A-F: CCACTCCTCCACCTTTGACG; ITM2A-R: CTGGTGGTCCAGGGGTCTTA; GAPDH-F: CTTTGAAAAGGGAATGACTGCTTAC; GAPDH-R: TACTAACATCACGAATTTCCTCCAC.

Western blotting

Western blot was performed according to our previous study [19]. In addition to RIPA buffer (Beyotime, Shanghai, China), 6× loading buffer (Transgene, Beijing, China), and protease and phosphatase inhibitors (Beyotime, Shanghai, China), the following primary antibodies were used: anti-ITM2A (106889-T40, 1:1000, Sino Biological Inc., China), anti-phosphorylated-STAT3 (Tyr705, 9145, 1:1000, Cell Signaling Technology, USA), anti-STAT3 (9139, 1:1000, Cell Signaling Technology, USA), anti-c-Myc (18583, 1:1000, Cell Signaling Technology, USA), and anti-Fibronectin (sc-8422, 1:1000, Santa Cruz, USA). The secondary antibodies were anti-mouse IgG (7076, 1:2000, Cell Signaling Technology, USA) and anti-rabbit IgG (7074, 1:2000, Cell Signaling Technology, USA) HRP linked antibodies.

Drug treatment

Recombinant human IL-6 (20 μg, Peprotech, USA), known as a STAT3 activator, was dissolved in PBS containing 5% trehalose. The working concentration of IL-6 was 100 ng/mL. PBS containing 5% trehalose was used as a control. Prior to experimentation, cells were subjected to a 24-hour starvation period, followed by the addition of IL-6 for subsequent assays.

Colony formation assay

1×10^3 BLCA cells were cultured in six-well plates with the completed medium. In 7 to 14 days, cells were washed twice with 1×PBS (Gibco, Carlsbad, CA, USA), fixed with 4% paraformaldehyde for 15 min, and stained with 0.1% crystal violet for 30 min. Divided adherent clones were counted with ImageJ.

5-Ethynyl-20-deoxyuridine (EdU) incorporation assay

4×10^4 BLCA cells with either ITM2A overexpression or knockdown were planted in 24-well plates. After the cells adhered to the wall, an EdU (Beyotime, Shanghai, China) incorporation assay was performed. T24 and UMUC-3 cells were treated with 10 μM EdU in the medium for 2.5 h, while SW780 cells were treated for 4 h. After fixing with 4% paraformaldehyde for 15 min, the cells were then incubated with a freshly made Click-iT reaction cocktail containing Azide 594 for 30 min at room temperature. Then the cells were stained with DAPI and observed under a confocal microscope.

Cell counting kit-8 (CCK-8) assay

A CCK-8 assay (Dojindo, Japan) was carried out for cell viability analysis. BLCA cells with either ITM2A overexpression or knockdown were inoculated in 96-well plates (3000 cells/well). The optical density value was assessed at 450 nm by a Multiskan Go plate reader (Beckman Coulter, Singapore) every 24 h.

Wound healing assay

A scratch assay was performed to determine the impact of ITM2A on the migratory ability of various cell groups. When the confluence of the pretreated cells reached 90%, they were incubated with serum-free medium containing mitomycin C (10 μg/mL, Sigma-Aldrich, St. Louis, MO, USA). Subsequently, monolayers were scratched with a 200-μL pipette tip and washed with 1×PBS. Photographs were taken at 0 h and 24 h, and then the wound width was measured and analyzed.

Transwell assay

Matrigel (BD Biosciences, San Jose, CA, USA) was diluted with PBS according to the manufacturer's protocol and added to the upper chambers of transwell inserts (Corning, NY, USA) at 100 μL/well. Then, 500 μL completed medium was added to each well of a 24-well plate. 3×10^4 cells were inoculated in each insert with 200 μL serum-free medium and incubated for 24 hours. The bottom of each insert was washed with PBS two times. After that, fixation

and staining methods of invaded cells were the same as the protocols of colony formation assay. Photographs were taken with Leica DMi8 and the invaded cells were counted with ImageJ.

Transcriptome sequencing

Total RNA was extracted by TRIzol reagent (Invitrogen, Carlsbad, CA, USA) according to the method previously described. The RNA samples were submitted to Sangon Biotechnology Co., Ltd. (Shanghai, China) for transcriptome sequencing after the evaluation of RNA integrity, quality, and quantity.

Xenograft experiments

4-week-old BALB/c male nude mice were purchased from Zhuhai BesTest Bio-Tech Company. All experimental procedures and protocols were reviewed and approved by Shenzhen TopBiotech Co., Ltd. Animal Center. Ten BALB/c nude mice were divided into two groups: Ctrl and ITM2A. After weighing, 3×10^6 transfected UMUC-3 cells were subcutaneously injected into the right underarm of the mice. Mice were killed 15 days after UMUC-3 cell inoculation. The xenograft tumors were weighed and prepared for RT-qPCR and western blot.

Statistical analysis

Data analysis was performed by GraphPad Prism 8 and SPSS 22. The results of three independent experiments were presented as mean ± standard deviation (SD). Student's independent t-test was taken for comparisons between two independent groups, while a one-way analysis of variance was used to evaluate significance among multiple groups. Pearson's chi-square test was performed for the categorical variables.

Results

Low expression of ITM2A was correlated with poor prognosis in bladder cancer

In our previous work, we utilized gene microarray technology to observe significantly lower expression of ITM2A in BLCA tissues compared to normal bladder tissues (Table S1). To further delineate the expression pattern of ITM2A in BLCA, we analyzed data from the TCGA and GEO databases. Notably, the mRNA level of ITM2A exhibited a marked decrease in BLCA tissues relative to normal bladder tissues (**Figure 1A-C**). Among the forty pairs of BLCA and adjacent normal bladder tissues, thirty-four cases exhibited lower ITM2A expression in BLCA tissues compared to adjacent normal bladder tissues (**Figure 1D**, **1E**). These results were further validated by tissue microarrays (**Figure 1F** and **Table 1**). Importantly, low ITM2A expression emerged as a significant indicator of poor prognosis for BLCA patients (**Figure 1G**). By analyzing clinicopathological characteristics, dysregulation of ITM2A in BLCA correlated with grade and AJCC stage (**Figure 1H**, **1I** and **Table 2**). The multivariate Cox regression analysis suggested that the patient's T stage and N stage were related to survival time (**Table 3**). In addition, BLCA cells (including SW780, T24, UMUC-3, J82, 5637, TCCSUP) displayed lower expression of ITM2A compared to the SV-HUC-1 cell line (**Figure 1J**, **1K**).

ITM2A inhibited the proliferation of BLCA cells in vitro

To further explore the biological function of ITM2A in BLCA, gain-of-function assays, and loss-of-function assays were conducted. T24 and UMUC-3 cells were infected with lentivirus carrying pLV-ITM2A (OE-ITM2A) for ITM2A overexpression, while two ITM2A-specific siRNAs were transfected into T24 and SW780 cells for ITM2A knockdown. The effectiveness of ITM2A modulation in BLCA cells was assessed through RT-qPCR and western blot analyses (**Figure 2A**, **2C**). The results of CCK-8 assays showed that the viability of BLCA cells with ITM2A overexpression was inhibited compared to the vector control group (**Figure 2B**). In contrast, the viability of BLCA cells with ITM2A knockdown was enhanced (**Figure 2D**). Overexpression of ITM2A inhibited the proliferation of T24 and UMUC-3 cells, while ITM2A knockdown exerted the opposite effect, as confirmed by colony formation assays and EdU incorporation assays (**Figures 2E**, **2F** and S1).

ITM2A restrained the migration and invasion of BLCA cells in vitro

To validate the suppressive effect of ITM2A on BLCA cell migration and invasion, wound healing assays and transwell assays were performed. Remarkable differences were observed

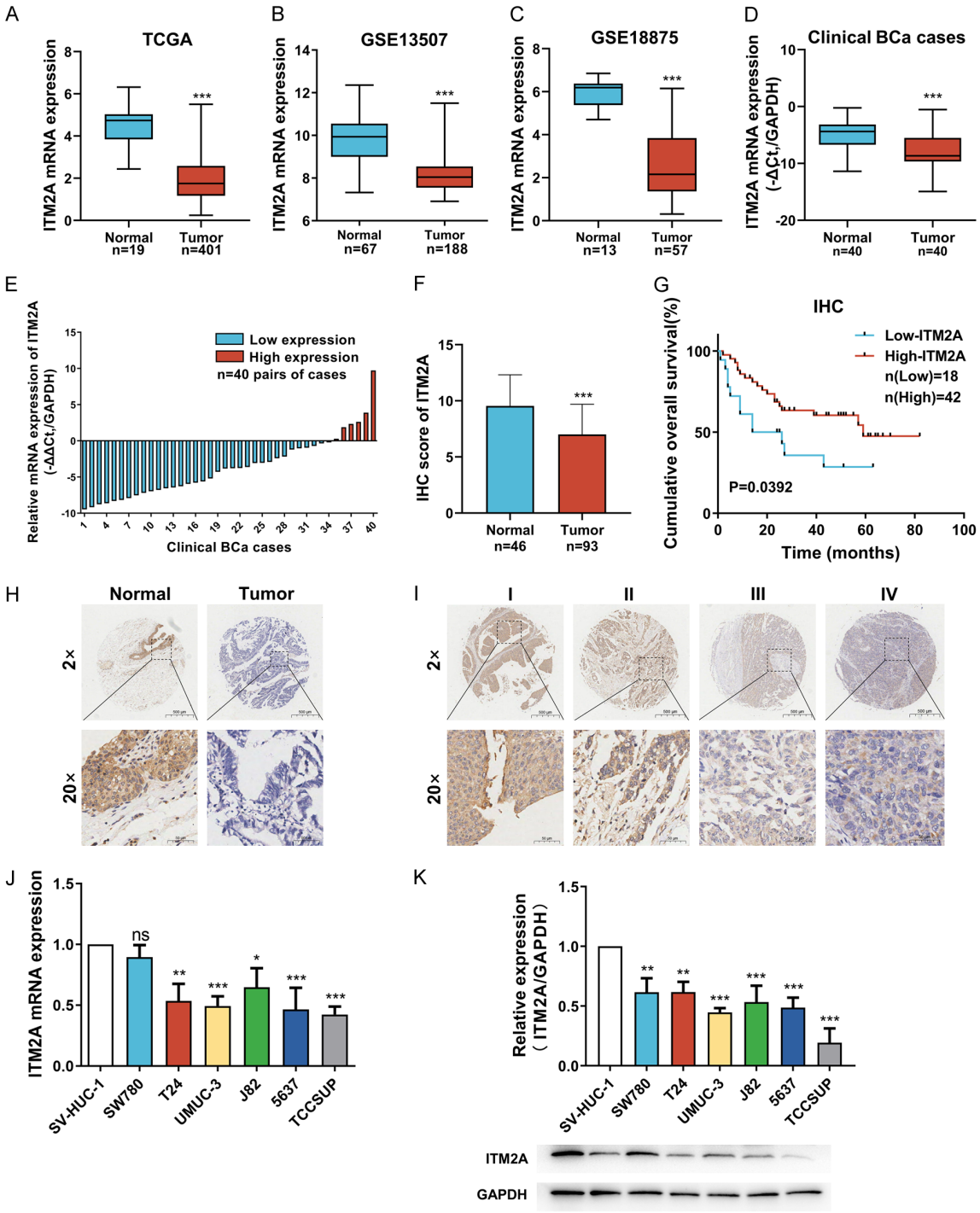

Figure 1. ITM2A expression was decreased in BLCA. A-C. The mRNA level of ITM2A in BLCA tissues and normal bladder tissues according to TCGA and GEO. D, E. The relative expression of ITM2A in forty pairs of BLCA tissues and adjacent normal bladder tissues. F. The relative expression of ITM2A in BLCA tissues and normal bladder tissues using IHC score. G. The expression of ITM2A was correlated with OS in IHC. H, I. ITM2A protein expression in different AJCC stages of BLCA tissues and adjacent normal bladder tissues in IHC assays. J, K. The expression of ITM2A in BLCA cell lines and SV-HUC-1 cells at both the transcriptional and translational levels. *P < 0.05, **P < 0.01, ***P < 0.001.

between the experimental group and control group cells. Restoration of ITM2A inhibited the migration and invasion abilities of BLCA cells (**Figure 3A**, **3C**), whereas knockdown of ITM2A

Table 1. Expression of ITM2A in cancer and normal bladder tissue (IHC)

	No. of cases	ITM2A expression		χ^2	*P*
		High	Low		
Bladder cancer	93	60	33	9.387	0.0022**
Normal bladder tissue	46	41	5		

Notes: *$P < 0.05$ or **$P < 0.01$ or ***$P < 0.001$ was considered significant (Chi-square test). IHC: immunohistochemistry staining.

Table 2. Correlation between ITM2A expression and clinicopathological characters of patients with bladder cancer (IHC)

Clinicopathological variables	No. of cases	ITM2A expression		χ^2	*P*
		Low	High		
All cases	63	21	42		
Gender				0.059	0.807
	Male	18	35		
	Female	3	7		
Age				0.027	0.868
	< 60	5	9		
	≥ 60	16	32		
Size				2.754	0.097
	≤ 5	19	27		
	> 5	1	10		
Grade					0.036*
	Low	0	7		
	High	20	33		
Pathologic T				6.206	0.102
	Ta-T1	3	13		
	T2	3	11		
	T3	12	13		
	T4	2	1		
Lymph node metastasis				0.003	0.957
	Negative	21	34		
	Positive	3	5		
AJCC stage				9.517	0.023*
	I	3	10		
	II	1	10		
	III	13	11		
	IV	3	5		

Notes: *$P < 0.05$ or **$P < 0.01$ or ***$P < 0.001$ was considered significant (Chi-square test or Fisher's exact test). IHC: immunohistochemistry staining.

conversely promoted these abilities (**Figure 3B**, **3D**).

ITM2A regulated the JAK2/STAT3 pathway in BLCA cells

To unravel the molecular mechanisms underlying ITM2A's role in BLCA progression, transcriptome sequencing was performed on BLCA cells with or without ITM2A overexpression in this study. Employing a cut-off criterion of $P < 0.05$ and $|\log_2$ fold-change (FC)$| \geq 2$, a volcano plot was generated (**Figure 4A**). Venn software identified 120 overlapping up-regulated genes and 92 overlapping down-regulated genes (**Figure 4B**). The 146 differentially expressed genes (DEGs) were depicted on the heat map (**Figure 4C**). To gain insights into the biological func-

Table 3. Multivariate Cox-regression analysis for patients after surgery (IHC)

Variate	*P*	Exp (B)	Low 95% CI	Up 95% CI
Gender	0.111	0.353	0.098	1.268
Age	0.251	0.502	0.155	1.628
Size	0.588	1.3	0.503	3.36
Grade	0.056	0.116	0.013	1.057
T	0.003*	11.832	2.296	60.963
N	0.004*	116.118	4.676	2883.551
AJCC	0.071	0.161	0.022	1.173
ITM2A	0.274	0.565	0.203	1.571

Notes: *$P < 0.05$ or **$P < 0.01$ or ***$P < 0.001$ was considered significant (Cox regression analysis). IHC: immunohistochemistry staining.

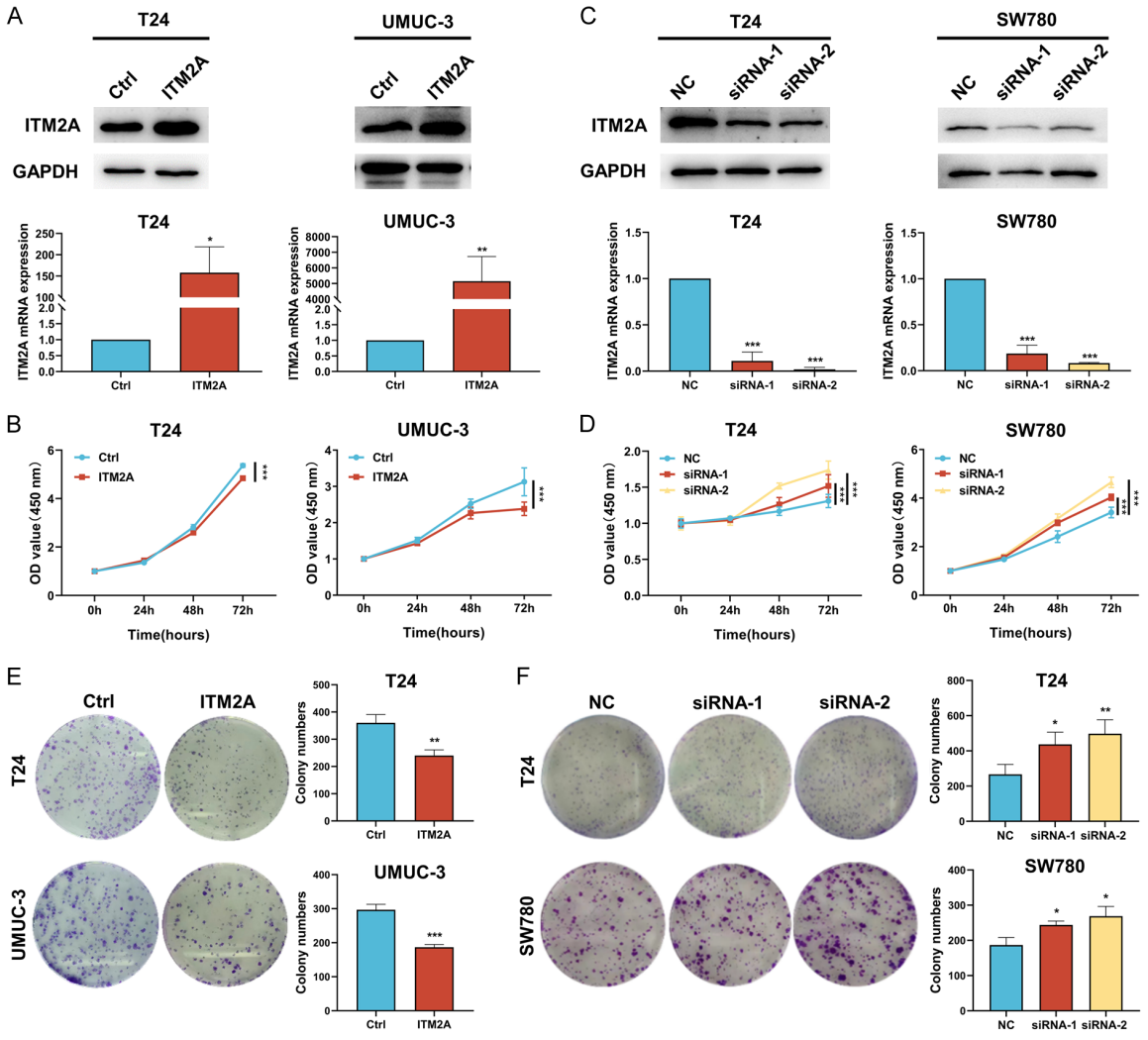

Figure 2. Upregulation of ITM2A inhibited the proliferation of BLCA cells. A. The transcriptional and translational levels of ITM2A in T24 and UMUC-3 cells after infection with empty vector or OE-ITM2A lentivirus. C. The transcriptional and translational levels of ITM2A in T24 and SW780 cells after transfection with siRNAs. B, D. CCK-8 assays showed the proliferation capacity of BLCA cells treated with the indicated lentivirus or siRNAs. E, F. Colony formation assays revealed the colony number of BLCA cells treated with the indicated lentivirus or siRNAs. Each experiment was repeated with three independent replicates.

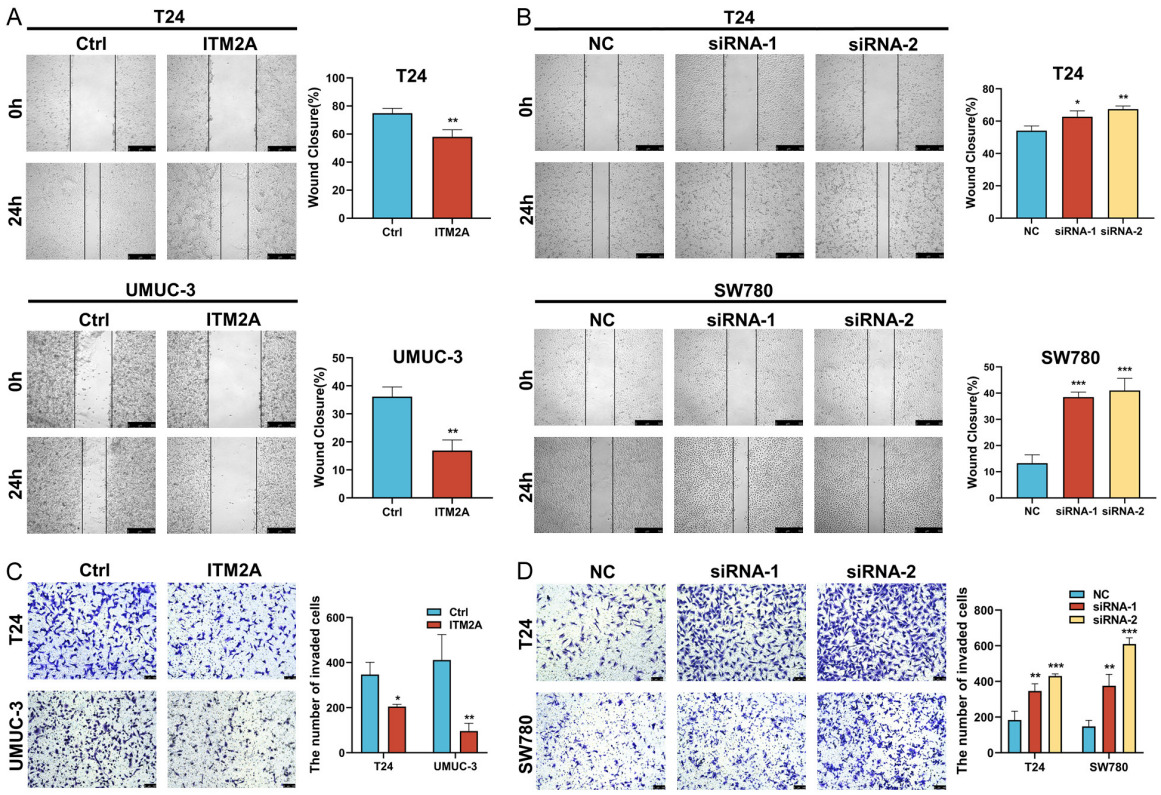

Figure 3. Upregulation of ITM2A inhibited the migration and invasion of BLCA cells. A, B. Wound healing assays showed the migration capacity of BLCA cells treated with the indicated lentivirus or siRNAs. C, D. Transwell assays revealed the invasion capacity of BLCA cells treated with the indicated lentivirus or siRNAs. Each experiment was repeated with three independent replicates.

tions of these significant DEGs, Gene Ontology (GO) and Kyoto Encyclopedia of Genes and Genomes (KEGG) pathway enrichment analysis were employed. The GO results suggested a significant enrichment of DEGs in growth and developmental process in biological process (BP), extracellular matrix and cell junction in cellular component (CC), blinding in molecular function (MF) (**Figure 4E**). Additionally, KEGG pathway enrichment analysis highlighted the top three pathways: the JAK/STAT signaling pathway, the ErbB signaling pathway, and the MAPK signaling pathway (**Figure 4D**, **4F**). Focusing on the JAK/STAT and MAPK signaling pathways for validation, our study identified significant differences in the phosphorylation expression of STAT3.

Protein analysis of BLCA cells showed that the ITM2A overexpressed group exhibited inactivation of the STAT3 signaling pathway, characterized by no change in total STAT3 levels but a notable decrease in phosphorylated STAT3 (**Figures 4G** and S2). We specifically focused on the tumor proliferation biomarker c-Myc and the migration and invasion biomarker FN1, both of which are downstream target genes of the STAT3 signaling pathway [20, 21]. The levels of c-Myc and FN1 expression were significantly decreased in the ITM2A overexpressed group (**Figures 4G** and S2).

Overexpression of ITM2A abolished the positive action of the STAT3 activator on the proliferation, migration, and invasion of BLCA cells

In a rescue experiment conducted on T24 and UMUC-3 cells treated with IL-6, we observed no significant change in ITM2A expression before and after the addition of IL-6. However, a notable increase in p-STAT3 levels was observed in the IL-6-treated groups compared to both the control group and the ITM2A overexpressed group. In parallel, the levels of c-Myc and FN1 were increased in response to IL-6 treatment (**Figures 5A** and S2). Compared with the vehicle group, IL-6 treatment led to an increase in BLCA cell viability, as confirmed by colony formation

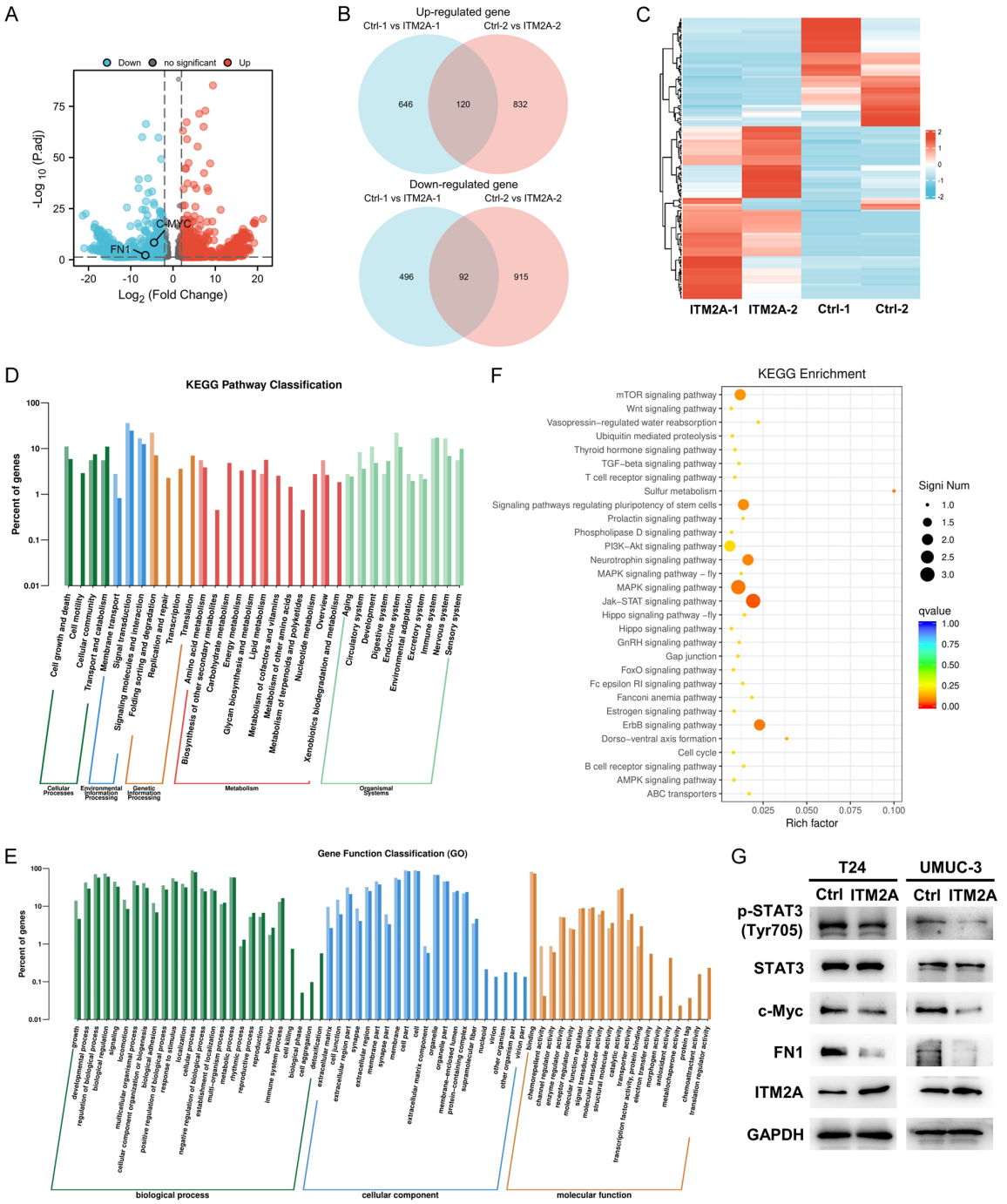

Figure 4. ITM2A was related to JAK2/STAT3 signaling pathway. A. Volcano plot of the distribution of DEGs by comparing Ctrl and OE-ITM2A cell samples. B. Venn diagram of upregulated genes and downregulated genes. C. Heatmap of RNA-seq expression data for BLCA cells infected with empty vector or OE-ITM2A lentivirus. D-F. The biological functions of DEGs were explored by GO and KEGG enrichment analysis. G. Western blot showed the expression of p-STAT3 (Tyr705), STAT3, c-Myc, FN1, and ITM2A in BLCA cells.

assays and EdU incorporation assays (**Figures 5B**, **5C** and S3). In addition, IL-6 promoted cell migration and invasion, while the ITM2A overexpressed group displayed the opposite effect (**Figure 5D** and **5E**).

ITM2A inhibited the growth of BLCA cells in vivo

To further investigate the relationship between ITM2A and the development of BLCA, UMUC-3

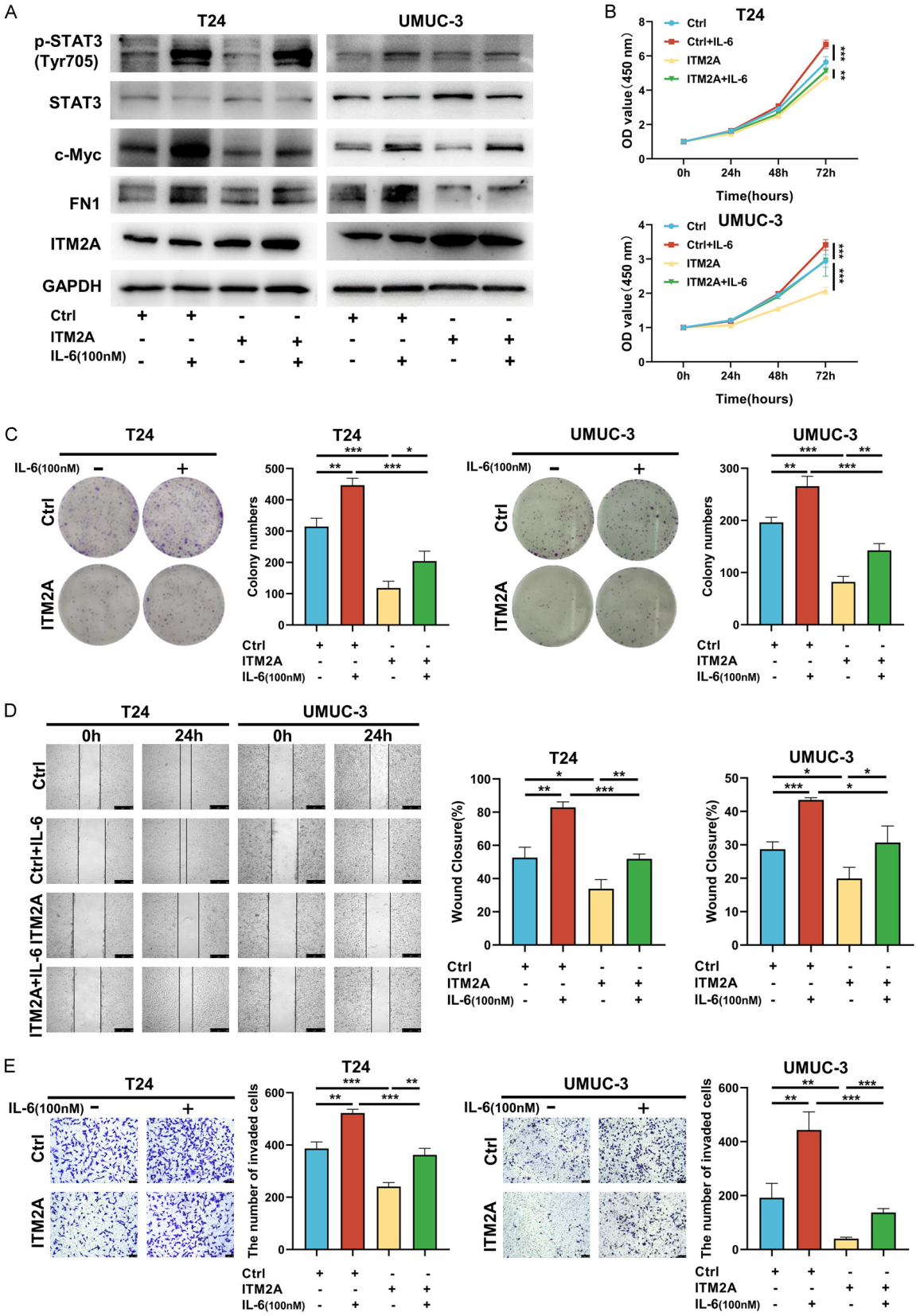

Figure 5. Overexpression of ITM2A abolished the positive action of the STAT3 activator on the growth of BLCA cells. A. Western blot showed the expression of p-STAT3 (Tyr705), STAT3, c-Myc, FN1, and ITM2A in T24 and UMUC-3 cells

treated with OE-ITM2A lentivirus and IL-6. B. CCK-8 assays showed the proliferation capacity of BLCA cells treated with OE-ITM2A lentivirus and IL-6. C. Colony formation assays revealed the colony number of BLCA cells treated with OE-ITM2A lentivirus and IL-6. D. Wound healing assays showed the migration capacity of BLCA cells treated with OE-ITM2A lentivirus and IL-6. E. Transwell assays revealed the invasive capacity of BLCA cells treated with OE-ITM2A lentivirus and IL-6. Each experiment was repeated with three independent replicates.

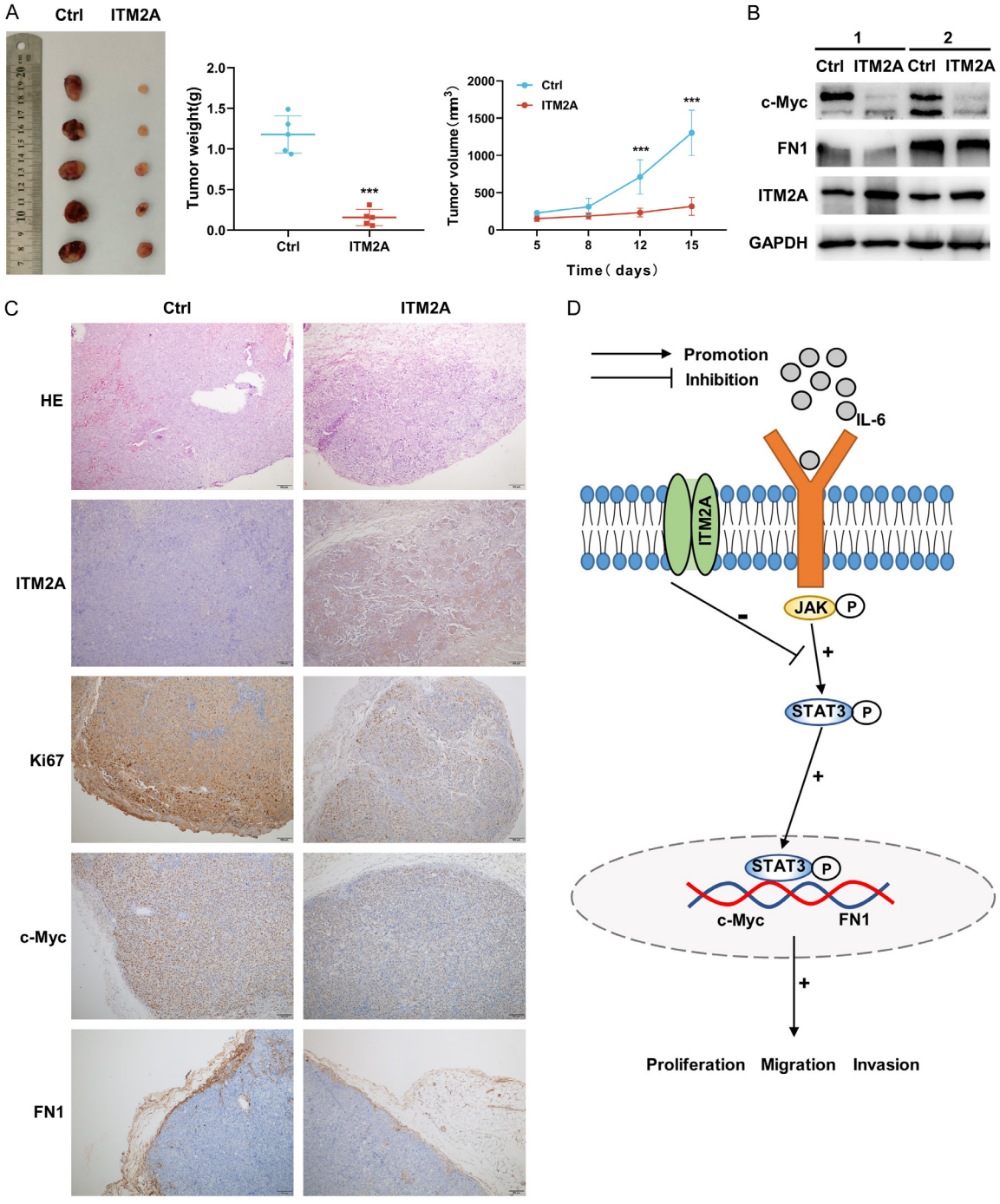

Figure 6. ITM2A inhibited the growth of BLCA cells in vivo. A. To develop a xenograft tumor model, subcutaneous injections of UMUC-3 cells infected with OE-ITM2A were administered to BALB/c mice (n=5 for each group). The tumor weight and volume were measured. B. The levels of c-Myc, FN1, and ITM2A were measured by western blot. C. The levels of ITM2A, Ki67, c-Myc, and FN1 were measured by IHC. D. Schematic diagram used to explain the role of ITM2A in BLCA.

cells stably infected with OE-ITM2A were injected subcutaneously into nude mice (n=5 for each group). Before the mice were sacrificed, tumor growth was markedly accelerated in the control group compared to the ITM2A overexpression group. Fifteen days post-inoculation, both tumor weight and volume were significantly decreased in the ITM2A overexpression group compared to the control group (**Figure 6A**). Moreover, the western blot analysis validated a substantial decrease in c-Myc and FN1 levels alongside a significant increase in ITM2A levels in the ITM2A overexpression group (**Figure 6B**). Additionally, the IHC assays demonstrated an increase in ITM2A expression and a decrease in Ki67, c-Myc, and FN1 expression following ITM2A overexpression (**Figure 6C**).

Discussion

This study highlighted crucial insights into ITM2A and its implications in BLCA. Firstly, our findings suggested a significant downregulation of ITM2A expression in BLCA tissues, and there was a clear correlation between reduced ITM2A levels and higher tumor grade, AJCC stage, and poorer overall survival time. Secondly, the restoration of ITM2A greatly inhibited cell proliferation, migration, and invasion, while the knockdown of ITM2A had opposing effects on BLCA cells. These findings aligned with the effects of ITM2A reported in previous studies on other tumors [15-18]. Importantly, while previous research on ITM2A primarily focused on bioinformatics analysis [22-25], our study provided a deeper understanding of ITM2A's mechanism in BLCA progression.

Transcriptome sequencing unveiled that ITM2A regulated BLCA by inhibiting the JAK2/STAT3 signaling pathway. The well-established role of STAT3 as a mediator in cytokine-driven signaling is crucial [26]. Some studies confirmed that STAT3 hyperactivation could significantly contribute to cancer cell growth and metastasis in BLCA [7]. This process involves transducing signals from cytokines, growth factors, and additional molecules in cancer, such as c-Myc and Bcl-X_L [5, 27]. In addition, previous evidence supported that GBP2 activated STAT3 through a certain pathway to induce the expression of FN1 [21], which encoded fibronectin, one of the most abundant and prevalent glycoproteins in the extracellular matrix [28]. By integrin-mediated signaling, FN1 influenced cell adhesion, migration, and development [29]. As the molecule downstream of STAT3, our observations indicated a decline in c-Myc and FN1 expression following ITM2A overexpression, suggesting that ITM2A's impact on BLCA cells was intricately linked to the STAT3 pathway.

Upon upregulating ITM2A, a significant reduction in p-STAT3 expression was noted, while differences in p-JAK2 and total JAK2 levels were not evident (Figure S4). Rescue experiments conducted with IL-6 reaffirmed that ITM2A's inhibition of p-STAT3 was a pivotal aspect of its impact on BLCA progression (**Figure 6D**).

In summary, our study suggested ITM2A as a tumor suppressor, exerting inhibitory effects on BLCA proliferation, migration, and invasion. Mechanistically, ITM2A regulated BLCA cell biological behavior by suppressing the activation of STAT3. While our study enhanced the understanding of BLCA development mechanisms, it also offered a promising avenue for BLCA treatment. However, certain limitations in our study warrant further investigation, particularly regarding the specific protein in the JAK2/STAT3 signaling pathway regulated by ITM2A. Further research into these aspects will provide a more comprehensive understanding in the future.

Acknowledgements

This study was supported by grants from the Sanming Project of Medicine in Shenzhen (No. SZSM202111007), the Science Technology and Innovation Commission of Shenzhen Municipality (No. JCYJ20220530150812027), and the Shenzhen High-level Hospital Construction Fund.

Disclosure of conflict of interest

None.

Abbreviations

BLCA, bladder cancer; NMIBC, nonmuscle-invasive bladder cancer; MIBC, muscle-invasive bladder cancer; TCGA, The Cancer Genome Atlas; GEO, Gene Expression Omnibus; FBS, fetal bovine serum; IHC, immunohistochemistry staining; RT-qPCR, reverse transcription-quantitative PCR; EdU, 5-Ethynyl-20-deoxyuridine; CCK-8, cell counting kit-8; DEG, differentially expressed gene; Go, Gene Ontology; KEGG, Kyoto Encyclopedia of Genes and Genomes.

Address correspondence to: Yan Wang, Department of Urology, Peking University Shenzhen Hospital, Institute of Urology, Shenzhen PKU-HKUST Medical Center, Shenzhen 518000, Guangdong, P. R. China. Tel: +86-0755-83923333; Fax: +86-0755-8392-3333; E-mail: wangyan198614@163.com; Bentao Shi, Department of Urology, The First Affiliated Hospital of Shenzhen University/Shenzhen Second People's Hospital, No. 3002, Sungangxi Road, Shenzhen 518035, Guangdong, P. R. China. Tel: +86-0755-83366388; Fax: +86-0755-83352843; E-mail: shibentaopku@126.com

References

[1] Sung H, Ferlay J, Siegel RL, Laversanne M, Soerjomataram I, Jemal A and Bray F. Global cancer statistics 2020: GLOBOCAN estimates of incidence and mortality worldwide for 36 cancers in 185 countries. CA Cancer J Clin 2021; 71: 209-249.

[2] Valenza C, Antonarelli G, Giugliano F, Aurilio G, Verri E, Briganti A, Curigliano G and Necchi A. Emerging treatment landscape of non-muscle invasive bladder cancer. Expert Opin Biol Ther 2022; 22: 717-734.

[3] Tolomeo M and Cascio A. The multifaced role of STAT3 in cancer and its implication for anticancer therapy. Int J Mol Sci 2021; 22: 603.

[4] Golus M, Bugajski P, Chorbińska J, Krajewski W, Lemiński A, Saczko J, Kulbacka J, Szydełko T and Małkiewicz B. STAT3 and its pathways' dysregulation-underestimated role in urological tumors. Cells 2022; 11: 3024.

[5] Li YJ, Zhang C, Martincuks A, Herrmann A and Yu H. STAT proteins in cancer: orchestration of metabolism. Nat Rev Cancer 2023; 23: 115-134.

[6] Wang HQ, Man QW, Huo FY, Gao X, Lin H, Li SR, Wang J, Su FC, Cai L, Shi Y, Liu B and Bu LL. STAT3 pathway in cancers: past, present, and future. MedComm (2020) 2022; 3: e124.

[7] Mirzaei S, Gholami MH, Mahabady MK, Nabavi N, Zabolian A, Banihashemi SM, Haddadi A, Entezari M, Hushmandi K, Makvandi P, Samarghandian S, Zarrabi A, Ashrafizadeh M and Khan H. Pre-clinical investigation of STAT3 pathway in bladder cancer: paving the way for clinical translation. Biomed Pharmacother 2021; 133: 111077.

[8] Korac-Prlic J, Degoricija M, Vilović K, Haupt B, Ivanišević T, Franković L, Grivennikov S and Terzić J. Targeting Stat3 signaling impairs the progression of bladder cancer in a mouse model. Cancer Lett 2020; 490: 89-99.

[9] Rengaraj D, Gao F, Liang XH and Yang ZM. Expression and regulation of type II integral membrane protein family members in mouse male reproductive tissues. Endocrine 2007; 31: 193-201.

[10] Pittois K, Wauters J, Bossuyt P, Deleersnijder W and Merregaert J. Genomic organization and chromosomal localization of the Itm2a gene. Mamm Genome 1999; 10: 54-56.

[11] Hedlund J, Johansson J and Persson B. BRICHOS - a superfamily of multidomain proteins with diverse functions. BMC Res Notes 2009; 2: 180.

[12] Namkoong S, Lee KI, Lee JI, Park R, Lee EJ, Jang IS and Park J. The integral membrane protein ITM2A, a transcriptional target of PKA-CREB, regulates autophagic flux via interaction with the vacuolar ATPase. Autophagy 2015; 11: 756-768.

[13] Van den Plas D and Merregaert J. In vitro studies on Itm2a reveal its involvement in early stages of the chondrogenic differentiation pathway. Biol Cell 2004; 96: 463-470.

[14] Davies SJ, Ryan J, O'Connor PBF, Kenny E, Morris D, Baranov PV, O'Connor R and McCarthy TV. Itm2a silencing rescues lamin A mediated inhibition of 3T3-L1 adipocyte differentiation. Adipocyte 2017; 6: 259-276.

[15] Zhang R, Xu T, Xia Y, Wang Z, Li X and Chen W. ITM2A as a tumor suppressor and its correlation with PD-L1 in breast cancer. Front Oncol 2021; 10: 581733.

[16] Zhou C, Wang M, Yang J, Xiong H, Wang Y and Tang J. Integral membrane protein 2A inhibits cell growth in human breast cancer via enhancing autophagy induction. Cell Commun Signal 2019; 17: 105.

[17] Nguyen TM, Shin IW, Lee TJ, Park J, Kim JH, Park MS and Lee EJ. Loss of ITM2A, a novel tumor suppressor of ovarian cancer through G2/M cell cycle arrest, is a poor prognostic factor of epithelial ovarian cancer. Gynecol Oncol 2016; 140: 545-553.

[18] Li Y, Wang J, Gao C, Hu Q and Mao X. Integral membrane protein 2A enhances sensitivity to chemotherapy via notch signaling pathway in cervical cancer. Bioengineered 2021; 12: 10183-10193.

[19] Xu J, Wang Y, Jiang J, Yin C and Shi B. ADAM12 promotes clear cell renal cell carcinoma progression and triggers EMT via EGFR/ERK signaling pathway. J Transl Med 2023; 21: 56.

[20] Turkson J. STAT proteins as novel targets for cancer drug discovery. Expert Opin Ther Targets 2004; 8: 409-422.

[21] Yu S, Yu X, Sun L, Zheng Y, Chen L, Xu H, Jin J, Lan Q, Chen CC and Li M. GBP2 enhances glioblastoma invasion through Stat3/fibronectin pathway. Oncogene 2020; 39: 5042-5055.

[22] Cao Z, Ao Y, Guo Y and Zhou S. Comprehensive analysis of mRNA expression profiles in head and neck cancer by using robust rank aggrega-

tion and weighted gene coexpression network analysis. Biomed Res Int 2020; 2020: 4908427.
[23] Zhao M, Huang W, Zou S, Shen Q and Zhu X. A five-genes-based prognostic signature for cervical cancer overall survival prediction. Int J Genomics 2020; 2020: 8347639.
[24] Meng H, Liu J, Qiu J, Nie S, Jiang Y, Wan Y and Cheng W. Identification of key genes in association with progression and prognosis in cervical squamous cell carcinoma. DNA Cell Biol 2020; 39: 848-863.
[25] Zhang Z, Li J, He T, Ouyang Y, Huang Y, Liu Q, Wang P and Ding J. The competitive endogenous RNA regulatory network reveals potential prognostic biomarkers for overall survival in hepatocellular carcinoma. Cancer Sci 2019; 110: 2905-2923.
[26] Wang Y, Shen Y, Wang S, Shen Q and Zhou X. The role of STAT3 in leading the crosstalk between human cancers and the immune system. Cancer Lett 2018; 415: 117-128.
[27] Kisseleva T, Bhattacharya S, Braunstein J and Schindler CW. Signaling through the JAK/STAT pathway, recent advances and future challenges. Gene 2002; 285: 1-24.
[28] Yamada KM and Olden K. Fibronectins–adhesive glycoproteins of cell surface and blood. Nature 1978; 275: 179-184.
[29] Xia S, Wang C, Postma EL, Yang Y, Ni X and Zhan W. Fibronectin 1 promotes migration and invasion of papillary thyroid cancer and predicts papillary thyroid cancer lymph node metastasis. Onco Targets Ther 2017; 10: 1743-1755.

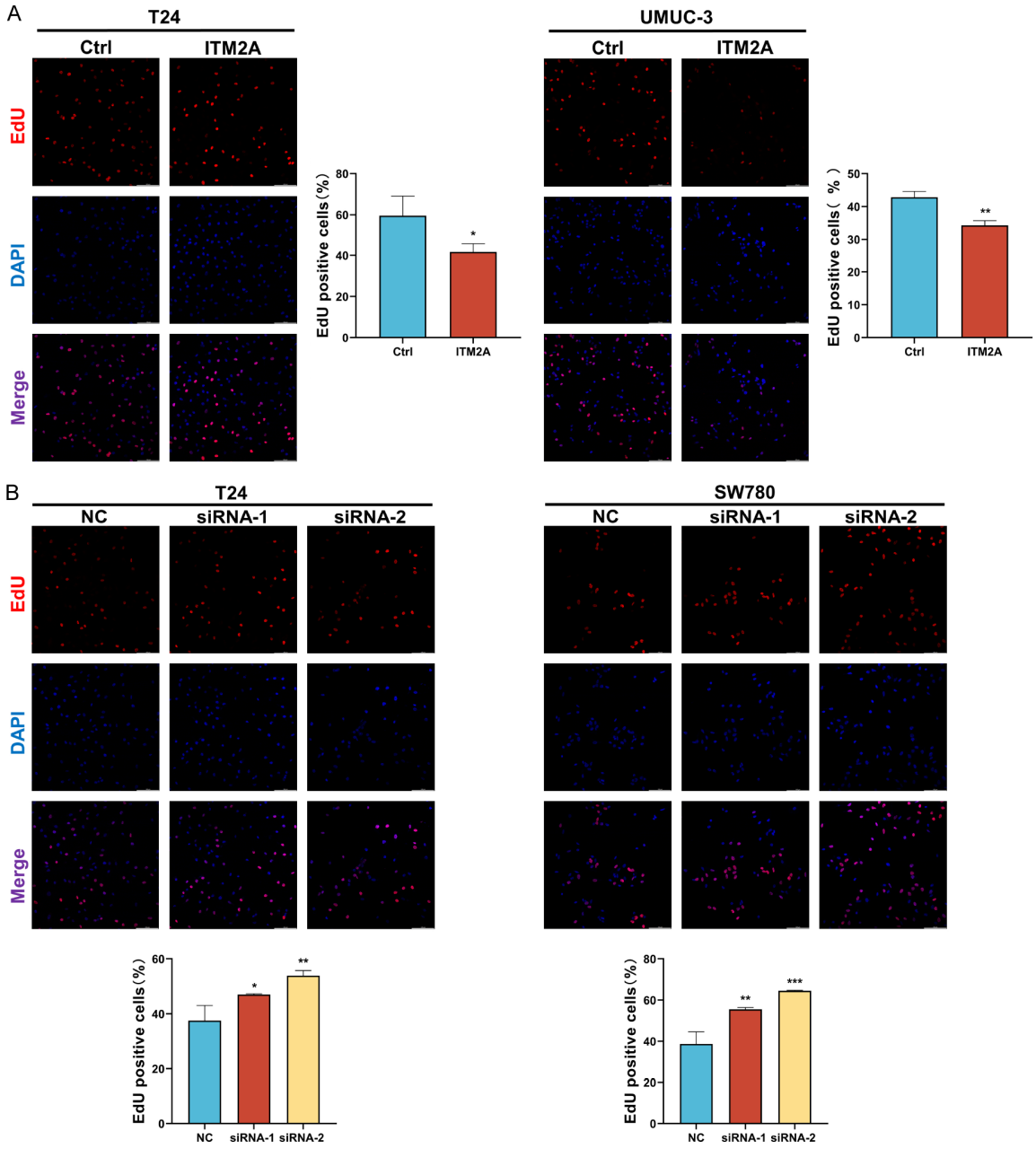

Figure S1. EdU incorporation assays demonstrated the proliferation capacity of BLCA cells treated with the indicated lentivirus or siRNAs.

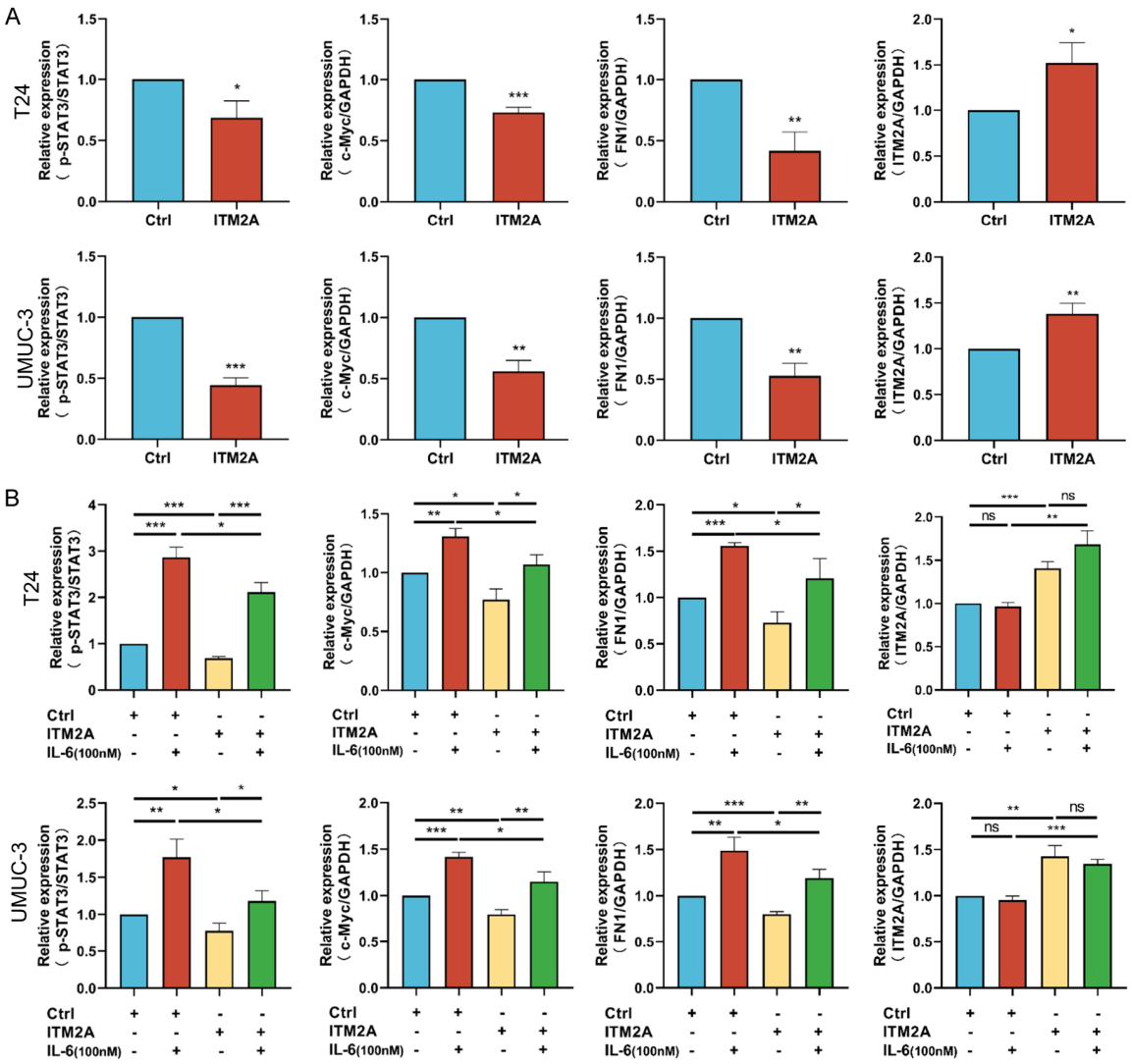

Figure S2. Western blotting analysis was done using the gray-scale image.

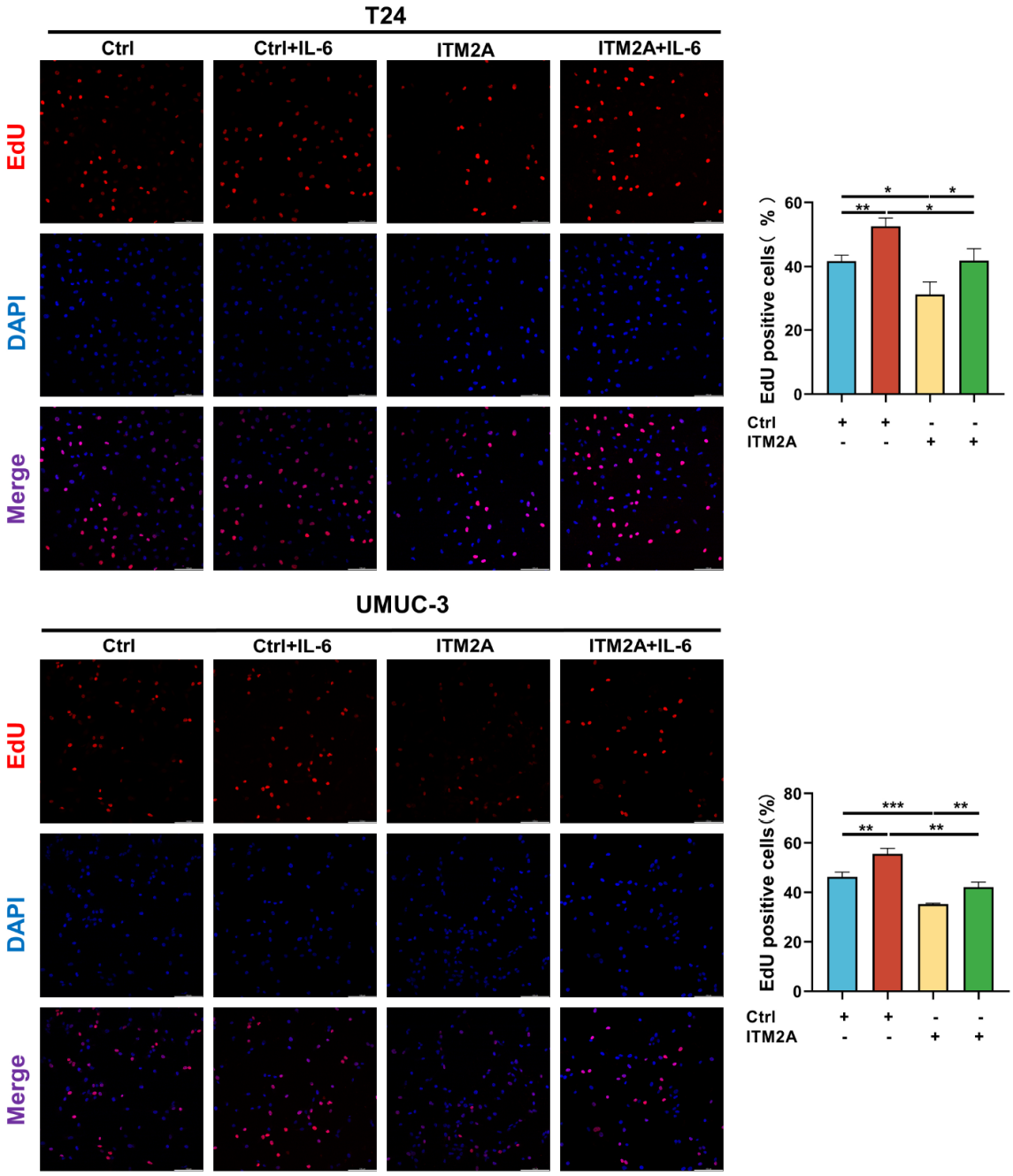

Figure S3. EdU incorporation assays demonstrated the proliferation capacity of BLCA cells treated with IL-6.

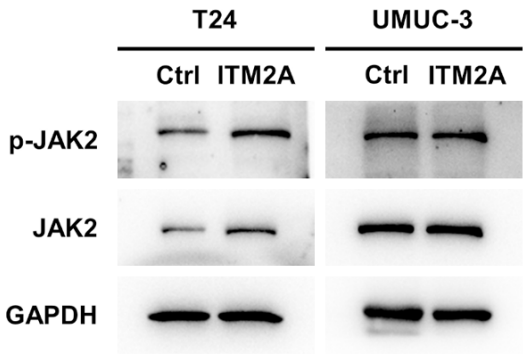

Figure S4. Western blot showed the expression of p-JAK2 and JAK2 in BLCA cells.